Cite as: C. M. Saad-Roy *et al.*, *Science* 10.1126/science.abg8663 (2021).

Epidemiological and evolutionary considerations of SARS-CoV-2 vaccine dosing regimes

Chadi M. Saad-Roy[1]*, Sinead E. Morris[2], C. Jessica E. Metcalf[3,4], Michael J. Mina[5], Rachel E. Baker[3,6], Jeremy Farrar[7], Edward C. Holmes[8], Oliver G. Pybus[9], Andrea L. Graham[3], Simon A. Levin[3], Bryan T. Grenfell[3,4,10]*, Caroline E. Wagner[11]*

[1]Lewis-Sigler Institute for Integrative Genomics, Princeton University, Princeton, NJ 08540, USA. [2]Department of Pathology and Cell Biology, Columbia University Medical Center, New York, NY 10032, USA. [3]Department of Ecology and Evolutionary Biology, Princeton University, Princeton, NJ 08544, USA. [4]Princeton School of Public and International Affairs, Princeton University, Princeton, NJ 08544, USA. [5]Departments of Epidemiology and Immunology and Infectious Diseases, Harvard School of Public Health, Boston, MA 02115, USA. [6]High Meadows Environmental Institute, Princeton University, Princeton, NJ 08544, USA. [7]The Wellcome Trust, London NW1 2BE, UK. [8]Marie Bashir Institute for Infectious Diseases and Biosecurity, School of Life and Environmental Sciences, and School of Medical Sciences, The University of Sydney, Sydney, NSW 2006, Australia. [9]Department of Zoology, University of Oxford, Oxford OX1 3SZ, UK. [10]Fogarty International Center, National Institutes of Health, Bethesda, MD 20892, USA. [11]Department of Bioengineering, McGill University, Montreal, QC H3A 0C3, Canada.

***Corresponding author. Email: csaadroy@princeton.edu (C.M.S.-R.); grenfell@princeton.edu (B.T.G.); caroline.wagner@mcgill.ca (C.E.W.)**

In the face of vaccine dose shortages and logistical challenges, various deployment strategies are being proposed to increase population immunity levels to SARS-CoV-2. Two critical issues arise: how will the timing of delivery of the second dose affect both infection dynamics and prospects for the evolution of viral immune escape via a build-up of partially immune individuals. Both hinge on the robustness of the immune response elicited by a single dose, compared to natural and two-dose immunity. Building on an existing immuno-epidemiological model, we find that in the short-term, focusing on one dose generally decreases infections, but longer-term outcomes depend on this relative immune robustness. We then explore three scenarios of selection and find that a one-dose policy may increase the potential for antigenic evolution under certain conditions of partial population immunity. We highlight the critical need to test viral loads and quantify immune responses after one vaccine dose, and to ramp up vaccination efforts throughout the world.

As the severe acute respiratory syndrome coronavirus 2 (SARS-CoV-2) betacoronavirus (β-CoV) pandemic continues, the deployment of safe and effective vaccines presents a key intervention for mitigating disease severity and spread and eventually relaxing non-pharmaceutical interventions (NPIs). At the time of writing, eleven vaccines have been approved by at least one country (*1*). We focus mainly on the vaccines from Pfizer/BioNTech, Moderna, and Oxford/AstraZeneca. The first two elicit adaptive immunity against SARS-CoV-2 in response to the introduction of messenger ribonucleic acid (mRNA) molecules that encode the spike protein of SARS-CoV-2 (*2*), and appear to offer greater than 95% (Pfizer/BioNTech (*3*), approved in 60 countries) and 94% (Moderna (*2*), approved in 38 countries) protection against symptomatic coronavirus disease 2019 (COVID-19). Both of these mRNA vaccines were tested in clinical trials according to a two-dose regime with dose spacing of 21 and 28 days for the Pfizer/BioNTech and Moderna platforms, respectively. The Oxford/AstraZeneca vaccine uses a non-replicating adenovirus vector, and has also been tested in clinical trials according to a two-dose regime with a target 28-day inter-dose period (although for logistical reasons some trial participants received their second dose after a delay of at least 12 weeks). Clinical trials indicated 62%–90% efficacy for this vaccine according to the specific dose administered (*4*). While we base our parameter choices and modeling assumptions on these three vaccines, our results are generalizable across platforms.

As these vaccines have been distributed internationally, several countries including the UK (*5*) and Canada (*6*) have chosen to delay the second dose in an effort to increase the number of individuals receiving at least one or in response to logistical constraints (*7*). Although a number of participants dropped out after a single dose of the vaccine in the Pfizer/BioNTech and Moderna trials, these studies were not designed to assess vaccine efficacy under such circumstances, and Pfizer has stated that there is no evidence that vaccine protection from a single dose extends beyond 21 days (*5*), although other data paint a more optimistic picture (*8*, *9*). The Oxford/AstraZeneca clinical trials did include different dose spacings, and limited evidence suggests that longer intervals (two to three months) did not affect and may even have improved vaccine efficacy (*4*, *5*). Ultimately, the consequences of deviating from manufacturer-prescribed dosing regimes at

the population scale remain unknown, but will hinge on immune responses.

While there has been significant progress in quantifying host immune responses following infection (*10*–*12*), substantial uncertainty regarding the strength and duration of both natural and vaccinal SARS-CoV-2 immunity remains. Previous work suggests that these factors will play a central role in shaping the future dynamics of COVID-19 cases (*13*). Future cases also create an environment for the selection of novel variants [e.g., (*14*–*16*)]. Of particular concern is the possibility of antigenic drift [e.g., for influenza (*17*), and (*18*) for the seasonal human coronavirus 229E] via immune escape from natural or vaccinal immunity. For example, immune escape might be especially important if vaccinal immunity elicited after the complete two-dose regime is highly protective whereas a single vaccine dose provides less effective immunity. Consequently, the longer term epidemiological and evolutionary implications of these different SARS-CoV-2 vaccine dosing regimes are not yet clear; the immediate need for effective mass vaccination makes understanding them critical to inform policy (*19*).

Here, we explore these epidemiological and evolutionary considerations with an extension of a recent immuno-epidemiological model for SARS-CoV-2 dynamics (*13*), depicted schematically in Fig. 1. Without vaccination, our model reduces to the Susceptible-Infected-Recovered-(Susceptible) [SIR(S)] model (*13*, *20*), where individual immunity after recovery from primary infection may eventually wane at rate δ, leading to potentially reduced susceptibility to secondary infections, denoted by the fraction ϵ relative to a baseline level of unity. This parameter ϵ is thus related to the (transmission-blocking) strength of immunity, and titrates between the SIR (lifetime immunity, $\epsilon = 0$) and SIRS (hosts regain complete susceptibility, $\epsilon = 1$) paradigms. Quantifying ϵ is challenging because it requires measuring reinfection rates after the waning of immunity. Some studies have made significant progress in this direction (*11*, *12*); however, uncertainties remain, particularly related to quantifying the average duration of immunity $1/\delta$. In this model extension (Fig. 1 and Materials and methods) we incorporate two vaccinated classes; V_1 accounts for individuals who have received one dose of a SARS-CoV-2 vaccine and V_2 tracks individuals who have received two doses. In the short term, we assume that both dosing options decrease susceptibility by fractions $\left(1-\epsilon_{V_1}\right)$ (one dose) and $\left(1-\epsilon_{V_2}\right)$ (two doses), inferred from the clinical trial data (though the nature of the infecting variant may influence this); we also assume that I_V tracks infection following vaccination. We allow for vaccinal immunity to wane at separate rates [ρ_1 (one dose) and ρ_2 (two doses)], moving individuals to the partially susceptible immune classes S_{S_1} and S_{S_2} characterized by (possibly different) levels of immune protection ϵ_1 and ϵ_2. Infection following waned one-dose or two-dose vaccinal immunity is tracked by the immune classes I_{S_1} and I_{S_2}, respectively. We consider a continuous spectrum for the inter-dose period $\left(\frac{1}{\omega}\right)$, with an infinite value corresponding to a "one-dose strategy", and model the rate of administration of the first dose ν as an increasing function of the inter-dose period (Fig. 1 and Materials and methods) to reflect the increase in available doses due to a delayed second dose. Thus, dosing regimes with longer inter-dose periods allow for higher coverage with the first dose.

We begin by projecting the epidemiological impacts of the different dosing regimes on medium-term temporal dynamics of COVID-19 cases. We then examine the potential evolutionary consequences of dosing regime by calculating a time-dependent relative net viral adaptation rate (*17*). This term is related to the strength of natural and vaccinal immunity (either via inducing selection through immune pressure or suppressing viral replication) as well as the sizes of classes of individuals experiencing infections after immune waning.

Epidemiological impacts

As a base case, we consider a high latitude European or North American city with initial conditions that qualitatively correspond to early 2021 (see supplementary materials and figs. S5 and S6 for other scenarios, e.g., a high initial attack rate or almost full susceptibility), in addition to a seasonal transmission rate (*21*) with NPIs (see Materials and methods). Note that given immunological and future control uncertainties, we are aiming to project qualitatively rather than formulate quantitative predictions for particular locations. The UK and Canadian policy is for a delayed second dose; they are not aiming for an "exclusively" one-dose policy. However, we explore the one-dose strategy as an extreme case for the "two-dose" vaccines; it also encompasses a pessimistic situation of waning public confidence in vaccination and individuals' own decisions to forgo the second dose. Finally, this one-dose policy could capture vaccines which only require a single dose, e.g., the Johnson & Johnson vaccine.

In Fig. 2, we present potential scenarios for medium-term SARS-CoV-2 infection and immunity dynamics contingent upon vaccine dosing regimes. We start by assuming that vaccination occurs at a constant rate, and assume a relatively optimistic maximum rate of administration of the first dose of $\nu_0 = 2\%$ of the population per week (see supplementary materials for other scenarios). Figure 2A and Fig. 2B correspond, respectively, to scenarios with weaker (and shorter) and stronger (and longer) natural and vaccinal adaptive immune responses. Thus, the former represents a scenario with higher secondary susceptible density than the latter. In each

panel, the top and bottom sections consider poor and robust one-dose vaccinal immunity, respectively. The leftmost column represents a one-dose vaccine policy (captured in the model by infinite dose spacing), with dose spacing decreasing to 4 weeks in the rightmost column (i.e., a strict two-dose policy with doses separated by the clinical trial window corresponding to Moderna's recommendations for their vaccine, hereafter referred to as the "recommended two-dose strategy").

As expected, we find that broader deployment of widely-spaced doses is beneficial. Specifically, a one-dose strategy (or a longer inter-dose period) may lead to a substantially reduced "first" epidemic peak of cases after the initiation of vaccination (compare the leftmost top panels of Fig. 2, A and B, with the no vaccination scenarios in fig. S1, A and B). This result applies even if immunity conferred by one vaccine dose is shorter and weaker than that following two-doses (top panels of Fig. 2, A and B). However under these conditions of imperfect immunity, an exclusively one-dose strategy then leads to an earlier subsequent peak due to the accumulation of partially susceptible individuals. When the rate of administration of the first dose is very high (fig. S4, ν_0 = 5% per week), this subsequent infection peak may be larger than that expected in the scenario with no vaccination. In general, the accumulation of partially susceptible individuals with waned one-dose vaccinal immunity can be mitigated by implementing a two-dose strategy and decreasing the time between doses. Thus, in situations of a less effective first dose where the second dose is delayed, it is important to ensure individuals eventually do obtain their second dose.

In line with intuition, longer and stronger immunity elicited after a single dose heightens the benefits of a one-dose strategy or of delaying the second dose (compare the top and bottom leftmost panels of Fig. 2, A and B). Additionally, the protective effects of adopting these strategies instead of the two-dose regime are maintained in the medium-term, with decreased burden in all future peaks. This is further summarized in Fig. 3A via the cumulative number of total and severe cases (right and left panels, respectively) over approximately four years from the time of vaccine initiation, normalized by the burdens with no vaccination; these ratios are plotted as a function of the inter-dose period and the one- to two-dose immune response ratio x_e (see figure caption for details). When the immune response conferred by a single dose is close to the robustness following two doses, total case numbers (Fig. 3A, right panel) can be substantially reduced by delaying the second dose. However, for smaller values of x_e, larger inter-dose periods are associated with more cases. The reduction in the cumulative burden of severe cases is even more sizeable (Fig. 3A, left panel) due to the assumed reduction in the fraction of severe cases for partially immune individuals. When vaccination rates are substantially lower (fig. S2, ν_0 = 0.1% per week; and fig. S3, ν_0 = 1% per week), the benefits of a single dose strategy diminish even for an effective first dose, as an insufficient proportion of the population are immunized. The short term effect of the vaccine on case numbers is sensitive to when it is introduced in the dynamical cycle (figs. S7 and S8), highlighting the critical interplay between the force of infection and the level of population immunity (see supplementary materials for further details).

Vaccines will be central to efforts to attain community immunity (*22*), and thus prevent local spread due to case importation. We therefore analytically calculated the first vaccine dose administration rate for a given inter-dose spacing required for community immunity in our model (see supplementary materials). In the long term, however, individuals whose one- or two-dose immunity has waned will likely be able to be vaccinated again before infection in countries with adequate supplies; we therefore incorporated re-vaccination of these individuals into the extended model and computed an analogous minimal vaccination rate which we plot in Fig. 3B. We find that as the inter-dose period grows, this minimal rate depends increasingly on the degree of reduction in susceptibility after the waning of one-dose vaccinal immunity ϵ_1 (Fig. 3B and see fig. S13 for other parameter choices). Vaccine refusal (*23*) may also impact the attainment of community immunity through vaccinal immunity in the longer-term (see supplementary materials).

Evolutionary impacts

The recent emergence of numerous SARS-CoV-2 variants in still relatively susceptible populations underline the virus's evolutionary potential (*24–26*). We focus here on the longer term potential for immune escape from natural or vaccinal immunity (*17*). For immune escape variants to spread within a population, they must first arise via mutation, and then there must be substantial selection pressure in their favor. We expect the greatest opportunity for variants to arise in (and spread from) hosts with the highest viral loads, likely those with the least immunity. On the other hand, we expect the greatest selection for escape where immunity is strongest. Previous research on the phylodynamic interaction between viral epidemiology and evolution (based on seasonal influenza) predicts that partially immune individuals (permitting intermediate levels of selection and transmission) could maximize levels of escape (*17*) (Fig. 4A). Under this model, we would project that different categories of secondarily infected people (after waning of natural immunity or immunity conferred from one or two doses of vaccine) would be key potential contributors to viral immune escape.

In Fig. 4, we consider three potential evolutionary scenarios, exploring different assumptions regarding viral abundance and within-host selection for the various immune classes. In all scenarios, we assume for simplicity that

immunity elicited after two doses of the vaccine is equivalent to that elicited after natural infection. We also assume that transmission rises with viral abundance in hosts (*17*). In Scenario I (black borders on circles, top panel of Fig. 4A), we assume that infections of all classes of partially susceptible individuals lead to strong selective pressures and low viral abundance (a marker of low transmission), and thus low rates of adaptation, with only slightly reduced immune pressure for infections after a waned single vaccine dose relative to natural infection or two doses. Scenario II (blue borders on circles, middle panel of Fig. 4A), considers a situation where natural and two-dose vaccinal immunity again lead to low viral abundance, but one-dose vaccinal immunity is associated with intermediate immune pressure that results in substantially higher rates of viral adaptation. Finally, in Scenario III (purple borders on circles, bottom panel of Fig. 4A), adaptive immune responses following waned natural, one dose, and two dose vaccinal immunity all lead to similar intermediate levels of immune pressure and high rates of viral adaptation. In all cases, we assume for tractability that viral immune escape is not correlated with clinical severity (*27*).

The relative potential viral adaptation rates [see (*17*) for more details] corresponding to each scenario are presented in the top rows of Fig. 4, B and C. This relative rate is estimated as the sum of the sizes of the infection classes following waned immunity (i.e., I_S after S_S, I_{S_1} after S_{S_1}, and I_{S_2} after S_{S_2}) weighted by the infection class-specific net viral adaptation rate assigned in each scenario. Therefore, this quantity reflects a weight-averaged potential rate for viral adaptation per-individual per-infection. The corresponding immune and susceptibility classes are plotted in the middle and bottom rows, respectively, according to the color scheme defined in Fig. 1A. The weaker immunity scenario of Fig. 2A is considered, with Fig. 4B and Fig. 4C corresponding, respectively, to the situations of a weaker and more robust single vaccine dose relative to two doses. The leftmost column corresponds to a one dose strategy, an inter-dose period of $\frac{1}{\omega} = 24$ weeks is assumed in the middle column, and the rightmost column assumes a two dose strategy with doses separated by the clinical trial window of $\frac{1}{\omega} = 4$ weeks.

Different assumptions regarding the strength and duration of adaptive immune responses to vaccines and natural infections alter projections for the proportions of individuals in the partially susceptible immune classes over time. When one dose vaccinal immunity is poor, a one-dose strategy results in the rapid accumulation of partially susceptible S_{S_1} individuals (Fig. 4B, bottom row) and a greater infection burden. (Note, this S_{S_1} immune class is highlighted in orange for visibility in Figs. 1, 2, and 4.) When the assumed individual rates of evolutionary adaptation arising from these infection classes are high (Scenarios II and III), we find that a one-dose strategy could lead to substantially higher relative rates of adaptation. This effect can be mitigated by implementing a two-dose strategy even with a longer inter-dose period than the recommended duration, echoing our epidemiological findings.

A single dose strategy of a strongly immunizing vaccine reduces infection rates, resulting in lower relative rates of adaptation when a one dose strategy is used; however the resulting large fraction of S_{S_1} individuals may still lead to evolutionary pressure, particularly when the potential viral adaptation rate associated with I_{S_1} infections is large. A two-dose strategy mitigates this effect, but the corresponding reduction in vaccinated individuals increases the infection burden from other classes. Thus, to avoid these potentially pessimistic evolutionary outcomes, our results highlight the importance of rapid vaccine deployment. More broadly, our results further underline the importance of equitable, global vaccination (*28*, *29*): immune escape anywhere will quickly spread.

Impact of increasing vaccination through time

In the supplementary materials (figs. S10 to S12), we explore the implications of ramping up vaccine deployment through two approaches. First, we examine a simple increase in the rate of administration of the first dose and unchanged dosing regimes (fig. S10). Qualitatively, these results are largely analogous to our previous results, and reflect the benefits of increasing population immunity through an increase in vaccination deployment.

However, as vaccines become more widely available, policies on dosing regimes may change. The second approach we consider is a timely shift to a two-dose policy with recommended inter-dose spacing as vaccine deployment capacity increases (figs. S11 and S12). Initially delaying (or omitting) the second dose decreases the first epidemic peak after the initiation of vaccination. Such a reduction in first peak size would also reduce secondary infections, and thus potentially immune escape in most cases (i.e., an evolutionary advantage). Subsequently, the switch to a manufacturer-timed vaccine dosage regime mitigates the potential medium-term disadvantages of delaying (or omitting) the second dose that may arise if immunity conferred from a single dose is relatively poor, including the accumulation of partially susceptible S_{S_1} individuals whose one-dose vaccinal immunity has waned. These contrasts highlight the importance of data-driven policies that undergo constant re-evaluation as vaccination progresses.

Caveats

Our immuno-epidemiological model makes several assumptions. While heterogeneities (superspreading, age, space, etc.) (*30*–*33*) are important for the quantitative prediction of SARS-CoV-2 dynamics, we previously found that these do not qualitatively affect our results (*13*). Nevertheless, we again briefly explore the epidemiological consequences of heterogeneities in transmission and vaccine coverage in the supplementary materials. We have also assumed that the robustness of immune responses following the second dose is independent of the inter-dose period, yet it is possible that delaying the second dose may actually enhance adaptive immune responses (*34*). Detailed clinical evaluation of adaptive immune responses after one and two vaccine doses with different inter-dose spacing is an important direction for future work.

Additionally, we have assumed highly simplified scenarios for NPIs. The chosen scenario was selected to qualitatively capture current estimates of SARS-CoV-2 prevalence and seropositivity in large cities. However, these values vary substantially between locations, a notable example being recent estimates of a large infection rate in Manaus, Brazil, during the first wave (*35*), or countries having almost no infections due to the successful implementation of NPIs (*36*–*38*). We have examined these scenarios in the supplementary materials (figs. S5 and S6). The qualitative projections of our model are sensitive to the composition of infection and immune classes at the onset of vaccination (including, therefore, the assumption of dramatically higher seropositivity levels, i.e., the sum of the S_S and R classes). We further explore this in the supplementary materials through the initiation of vaccination at different times in the dynamic cycle (figs. S7 and S8). Thorough explorations of various NPIs, seasonal transmission rate patterns, vaccine deployment rates, dosing regimes, and clinical burdens can be investigated for broad ranges of epidemiological and immunological parameters with the online interactive application, available at (*39*).

Finally, we have explored the simplest evolutionary model, which can only give a general indication of the potential for evolution under different scenarios. Including more complex evolutionary models (*40*, *41*) into our framework is thus another important area for future work. Population heterogeneities likely have complex impacts on viral evolution. First, heterogeneities in immune responses and transmission (e.g., chronically infected hosts that shed virus for extended periods (*42*), or focused versus polyclonal responses) may have important impacts on the accumulation of genetic diversity and the strength of selection pressures, and hence on evolutionary potential [e.g., for influenza, see (*43*)]. Second, there are complex evolutionary implications of disease severity minimization by vaccination (*27*, *44*). Third, superspreading and contact structure could influence the rate of spread of novel variants through a population (*45*). Additionally, increases in viral avidity to the human ACE2 receptor might generate multiple benefits for the virus in terms of enhanced transmission and immune escape (*46*). Finally, genetic processes such as clonal interference, epistasis, and recombination also add substantial complexity to evolutionary dynamics [e.g., (*17*, *47*, *48*)]. Further model refinements should also include these details for increased accuracy. A full list of caveats is presented in the supplementary materials.

Conclusion

The deployment of SARS-CoV-2 vaccines in the coming months will strongly shape post-pandemic epidemiological trajectories and characteristics of accumulated population immunity. Dosing regimes should seek to navigate existing immunological and epidemiological trade-offs between individuals and populations. Using simple models, we have shown that different regimes may have crucial epidemiological and evolutionary impacts, resulting in a wide range of potential outcomes in the medium term. Our work also lays the foundation for a number of future considerations related to vaccine deployment during ongoing epidemics, especially preparing against future pandemics.

In line with intuition, spreading single doses in emergency settings (i.e., rising infections) is beneficial in the short term and reduces prevalence. Furthermore, we find that if immunity following a single dose is robust, then delaying the second dose is also optimal from an epidemiological perspective in the longer term. On the other hand, if one-dose vaccinal immunity is weak, the outcome could be more pessimistic; specifically, a vaccine strategy with a very long inter-dose period could lead to marginal short-term benefits (a decrease in the short-term burden) at the cost of a higher infection burden in the long term and substantially more potential for viral evolution. These negative longer term effects may be alleviated by the eventual administration of a second dose, even if it is moderately delayed. With additional knowledge of the relative strength and duration of one-dose vaccinal immunity and corresponding, clinically-informed policies related to dosing regimes, pessimistic scenarios may be avoided. For context, at the time of writing, the UK for example has been particularly successful in rolling out vaccination to a large population with a wide spacing between doses (*49*). Our model illustrates that, ultimately, the long term impacts of this strategy, especially in terms of transmission and immune escape, will depend on the duration and strength of one-dose vaccinal immunity. Recent experience of weaker vaccinal immunity against the B.1.351 strain (*50*) underlines the importance of both detecting novel strains and titrating the strength of natural and vaccinal immunity against them.

In places where vaccine deployment is delayed and vaccination rates are low, our results stress the subsequent

negative epidemiological and evolutionary impacts that may emerge. Particularly since these consequences (e.g., the evolution of new variants) could emerge as global problems, this underlines the urgent need for global equity in vaccine distribution and deployment (*28*, *29*).

Current uncertainties surrounding the strength and duration of adaptive immunity in response to natural infection or vaccination lead to very broad ranges for the possible outcomes of various dosing regimes. Nevertheless, ongoing elevated COVID-19 case numbers stresses the rapid need for effective, mass vaccine deployment. Overall, our work emphasizes that the impact of vaccine dosing regimes are strongly dependent on the relative robustness of immunity conferred by a single dose. It is therefore imperative to determine the strength and duration of clinical protection and transmission-blocking immunity through careful clinical evaluations (including, for instance, randomized control trials of dose intervals and regular testing of viral loads in vaccinated individuals, their contacts, and those who have recovered from natural infections) in order to enforce sound public policies. More broadly, our results underscore the importance of exploring the phylodynamic interaction of pathogen dynamics and evolution, from within host to global scales, for SARS-CoV-2, influenza, and other important pathogens (*40*, *41*, *47*, *48*, *51*, *52*).

Materials and methods

Model formulation

We extend the model of (*13*) to examine different vaccination strategies. The additional compartments are as follows: V_i denotes individuals vaccinated with i doses and are thus immune; S_{S_i} denotes individuals whose complete i-dose immunity has waned and are now partially susceptible again; I_{S_i} denotes individuals who were in S_{S_i} and have now been infected again; I_V denotes individuals for whom the vaccine did not prevent infection.

The extended model contains several new parameters: $\frac{1}{\rho_i}$ is the average duration of vaccinal immunity V_i; $\frac{1}{\omega}$ is the average inter-dose period; ϵ_{V_i} is the decrease in susceptibility following vaccination with dose i; ϵ_i is the decrease in susceptibility following waning of i-dose immunity; α_i is the relative infectiousness of individuals in I_{S_i}; and α_V is the relative infectiousness of individuals in I_V. To allow for heterogeneity in vaccinal immune responses and potentially cumulative effects of natural and vaccinal immunity, we take c to be the fraction of previously-infected partially susceptible individuals (S_S) for whom one dose of the vaccine gives equivalent immunity to two-doses for fully susceptible individuals (S_P). Finally, x_i is the fraction of individuals in S_{S_i} that are re-vaccinated, and (1-p_i) is the fraction of individuals in S_{S_i} for whom re-administration of the "first dose" provides equivalent immune protection to two doses (i.e., they transition to the V_2 class). The full set of equations governing the transitions between these infection and immunity classes is then given by

$$\frac{dS_P}{dt} = \mu - \beta S_P\left[I_P + \alpha I_S + \alpha_V I_V + \alpha_1 I_{S_1} + \alpha_2 I_{S_2}\right] - \left(S_{\text{vax}}\nu + \mu\right)S_P \quad (1a)$$

$$\frac{dI_P}{dt} = \beta S_P\left[I_P + \alpha I_S + \alpha_V I_V + \alpha_1 I_{S_1} + \alpha_2 I_{S_2}\right] - \left(\gamma + \mu\right)I_P \quad (1b)$$

$$\frac{dR}{dt} = \gamma\left(I_P + I_s + I_V + I_{S_1} + I_{S_2}\right) - \left(\delta + \mu\right)R \quad (1c)$$

$$\frac{dS_S}{dt} = \delta R - \epsilon\beta S_S\left[I_P + \alpha I_S + \alpha_V I_V + \alpha_1 I_{S_1} + \alpha_2 I_{S_2}\right] - \left(S_{\text{vax}}\nu + \mu\right)S_S \quad (1d)$$

$$\frac{dI_S}{dt} = \epsilon\beta S_S\left[I_P + \alpha I_S + \alpha_V I_V + \alpha_1 I_{S_1} + \alpha_2 I_{S_2}\right] - \left(\gamma + \mu\right)I_S \quad (1e)$$

$$\frac{dV_1}{dt} = s_{\text{vax}}\nu S_P + c s_{\text{vax}}\nu S_S + x_1 P_1 s_{\text{vax}}\nu S_{S_1} + x_2 P_2 s_{\text{vax}}\nu S_{S_2} - \epsilon_{V_1}\beta V_1\left[I_P + \alpha I_S + \alpha_V I_V + \alpha_1 I_{S_1} + \alpha_2 I_{S_2}\right] - \left(\omega + \rho_1 + \mu\right)V_1 \quad (1f)$$

$$\frac{dV_2}{dt} = \left(1-c\right)s_{\text{vax}}\nu S_S + x_1\left(1-p_1\right)s_{\text{vax}}\nu S_{S_1} + x_2\left(1-p_2\right)s_{\text{vax}}\nu S_{S_2} + \omega V_1 - \epsilon_{V_2}\beta V_2\left[I_P + \alpha I_S + \alpha_V I_V + \alpha_1 I_{S_1} + \alpha_2 I_{S_2}\right] - \left(\rho_2 + \mu\right)V_2 \quad (1g)$$

$$\frac{dI_V}{dt} = \beta\left(\epsilon_{V_1}V_1 + \epsilon_{V_2}V_2\right)\left[I_P + \alpha I_S + \alpha_V I_V + \alpha_1 I_{S_1} + \alpha_2 I_{S_2}\right] - \left(\gamma - \mu\right)I_V \quad (1h)$$

$$\frac{dS_{S_1}}{dt} = P_1 V_1 - \epsilon_1\beta S_{S_1}\left[I_P + \alpha I_S + \alpha_V I_V + \alpha_1 I_{S_1} + \alpha_2 I_{S_2}\right] - \left(s_{\text{vax}}x_1\nu + \mu\right)S_{S_1} \quad (1i)$$

$$\frac{dS_{S_2}}{dt} = P_2 V_2 - \epsilon_2\beta S_{S_2}\left[I_P + \alpha I_S + \alpha_V I_V + \alpha_1 I_{S_1} + \alpha_2 I_{S_2}\right] - \left(s_{\text{vax}}x_2\nu + \mu\right)S_{S_2} \quad (1j)$$

$$\frac{dI_{S_1}}{dt} = \epsilon_1\beta S_{S_1}\left[I_P + \alpha I_S + \alpha_V I_V + \alpha_1 I_{S_1} + \alpha_2 I_{S_2}\right] - \left(\gamma + \mu\right)I_{S_1} \quad (1k)$$

$$\frac{dI_{S_2}}{dt} = \epsilon_2\beta S_{S_2}\left[I_P + \alpha I_S + \alpha_V I_V + \alpha_1 I_{S_1} + \alpha_2 I_{S_2}\right] - \left(\gamma + \mu\right)I_{S_2} \quad (1l)$$

For all simulations, we take $\mu = 0.02\ y^{-1}$ corresponding to a yearly crude birth rate of 20 per 1000 people. Additionally, we take the infectious period to be $1/\gamma = 5$ days, consistent with the modeling in (*13*, *21*, *53*) and the estimation of a serial interval of 5.1 days for COVID-19 in (*54*), and assume that $c = 0.5$. We take the relative transmissibility of infections to be $\alpha = \alpha_V = \alpha_1 = \alpha_2 = 1$, and therefore only modulate the relative susceptibility to disease ϵ. For the initial conditions of all simulations, we take $I_P = 1 \times 10^{-9}$ and assume the remainder of the population is in the fully susceptible class. The values of the remaining parameters used in the various simulations are specified throughout the main text.

Determination of seasonal reproduction numbers

In order to reflect observed seasonal variation in transmission rates for respiratory infections arising from related coronaviruses (*21*), influenza (*21*) and respiratory syncytial virus (*55*), we base seasonal reproduction numbers in this work on those in (*13*), which were calculated in (*21*) based on the climate of New York City. Other seasonal patterns can be explored using the interactive online application. In all simulations, we modify these values to force a mean value for the basic reproduction number of $\overline{R}_0 = \langle R_0(t) \rangle = 2.3$ by multiplying the climate-derived time series $R_{0,c}(t)$ by 2.3 and dividing by its average value, i.e.

$$R_0(t) = R_{0,c}(t)\frac{2.3}{\overline{R}_{0,c}}$$

Modeling of nonpharmaceutical interventions (NPIs)

In all simulations, we enforce periods of NPI adoption (arising from behaviors and policies such as lock downs, mask-wearing, and social distancing) in which the transmission rate is reduced from its seasonal value described in the previous section. In particular, we assume that NPIs are adopted between weeks 8 and 47 following the pandemic onset resulting in the transmission rate being reduced to 45% of its seasonal value. Between weeks 48 and 79, we assume that the transmission rate is to 30% higher than the previous time interval (reflecting an overall reduction to 45(1.3) = 58.5% of the original transmission rate), due to either behavioral changes following the introduction of the vaccine or the emergence of more transmissible strains. Finally, we assume that NPIs are completely relaxed beyond week 80.

Linking vaccination rate to inter-dose period

We consider an exponential relationship between the rate of administration of the first vaccination dose $\nu[\omega]$ and the inter-dose period $\frac{1}{\omega}$. We assume that this rate is maximized at ν_0 when no second dose occurs (i.e., $\omega = 0$, an infinite inter-dose period), and that when the first and second doses are spaced by the clinically recommended inter-dose period L_{opt} $\left(\omega_{\text{opt}} = \frac{1}{L_{\text{opt}}}\right)$, the rate of administration of the first dose is one half of its maximum value. Thus, $\nu[\omega] = 2^{-L_{\text{opt}}\omega}\nu_0$.

REFERENCES AND NOTES

1. McGill COVID19 Vaccine Tracker Team, COVID19 Vaccine Tracker; https://covid19.trackvaccines.org/vaccines/.
2. L. R. Baden, H. M. El Sahly, B. Essink, K. Kotloff, S. Frey, R. Novak, D. Diemert, S. A. Spector, N. Rouphael, C. B. Creech, J. McGettigan, S. Khetan, N. Segall, J. Solis, A. Brosz, C. Fierro, H. Schwartz, K. Neuzil, L. Corey, P. Gilbert, H. Janes, D. Follmann, M. Marovich, J. Mascola, L. Polakowski, J. Ledgerwood, B. S. Graham, H. Bennett, R. Pajon, C. Knightly, B. Leav, W. Deng, H. Zhou, S. Han, M. Ivarsson, J. Miller, T. Zaks; COVE Study Group, Efficacy and safety of the mRNA-1273 SARS-CoV-2 vaccine. *N. Engl. J. Med.* **384**, 403–416 (2021). doi:10.1056/NEJMoa2035389 Medline
3. F. P. Polack, S. J. Thomas, N. Kitchin, J. Absalon, A. Gurtman, S. Lockhart, J. L. Perez, G. Pérez Marc, E. D. Moreira, C. Zerbini, R. Bailey, K. A. Swanson, S. Roychoudhury, K. Koury, P. Li, W. V. Kalina, D. Cooper, R. W. Frenck Jr., L. L. Hammitt, Ö. Türeci, H. Nell, A. Schaefer, S. Ünal, D. B. Tresnan, S. Mather, P. R. Dormitzer, U. Şahin, K. U. Jansen, W. C. Gruber; C4591001 Clinical Trial Group, Safety and efficacy of the bnt162b2 mRNA Covid-19 vaccine. *N. Engl. J. Med.* **383**, 2603–2615 (2020). doi:10.1056/NEJMoa2034577 Medline
4. M. Voysey, S. A. C. Clemens, S. A. Madhi, L. Y. Weckx, P. M. Folegatti, P. K. Aley, B. Angus, V. L. Baillie, S. L. Barnabas, Q. E. Bhorat, S. Bibi, C. Briner, P. Cicconi, A. M. Collins, R. Colin-Jones, C. L. Cutland, T. C. Darton, K. Dheda, C. J. A. Duncan, K. R. W. Emary, K. J. Ewer, L. Fairlie, S. N. Faust, S. Feng, D. M. Ferreira, A. Finn, A. L. Goodman, C. M. Green, C. A. Green, P. T. Heath, C. Hill, H. Hill, I. Hirsch, S. H. C. Hodgson, A. Izu, S. Jackson, D. Jenkin, C. C. D. Joe, S. Kerridge, A. Koen, G. Kwatra, R. Lazarus, A. M. Lawrie, A. Lelliott, V. Libri, P. J. Lillie, R. Mallory, A. V. A. Mendes, E. P. Milan, A. M. Minassian, A. McGregor, H. Morrison, Y. F. Mujadidi, A. Nana, P. J. O'Reilly, S. D. Padayachee, A. Pittella, E. Plested, K. M. Pollock, M. N. Ramasamy, S. Rhead, A. V. Schwarzbold, N. Singh, A. Smith, R. Song, M. D. Snape, E. Sprinz, R. K. Sutherland, R. Tarrant, E. C. Thomson, M. E. Török, M. Toshner, D. P. J. Turner, J. Vekemans, T. L. Villafana, M. E. E. Watson, C. J. Williams, A. D. Douglas, A. V. S. Hill, T. Lambe, S. C. Gilbert, A. J. Pollard; Oxford COVID Vaccine Trial Group, Safety and efficacy of the ChAdOx1 nCoV-19 vaccine (AZD1222) against SARS-CoV-2: An interim analysis of four randomised controlled trials in Brazil, South Africa, and the UK. *Lancet* **397**, 99–111 (2021). doi:10.1016/S0140-6736(20)32661-1 Medline
5. G. Iacobucci, E. Mahase, Covid-19 vaccination: What's the evidence for extending the dosing interval? *BMJ* **372**, n18 (2021). doi:10.1136/bmj.n18 Medline
6. "Quebec opts to delay 2nd dose of vaccine in order to immunize health-care workers faster," CBC News, 5 January 2021; www.cbc.ca/news/canada/montreal/quebec-second-vaccine-dose-delays-1.5861194.
7. M. Rabson, "Provinces delaying or revisiting vaccine programs as Pfizer slows dose deliveries," CTV News, 18 January 2021; www.ctvnews.ca/health/coronavirus/provinces-delaying-or-revisiting-vaccine-programs-as-pfizer-slows-dose-deliveries-1.5271829.
8. G. Chodcik, L. Tene, T. Patalon, S. Gazit, A. Ben-Tov, D. Cohen, K. Muhsen, The effectiveness of the first dose of BNT162b2 vaccine in reducing SARS-CoV-2 infection 13-24 days after immunization: real-world evidence. medRxiv 2021.01.27.21250612 [Preprint]. 29 January 2021. https://doi.org/10.1101/2021.01.27.21250612.
9. V. J. Hall, S. Foulkes, A. Saei, N. Andrews, B. Oguti, A. Charlett, E. Wellington, J. Stowe, N. Gillson, A. Atti, J. Islam, I. Karagiannis, K. Munro, J. Khawam, The SIREN Study Group, M. A. Chand, C. Brown, M. E. Ramsay, J. L. Bernal, S. Hopkins, Effectiveness of BNT162b2 mRNA vaccine against infection and COVID-19 vaccine coverage in healthcare workers in England, multicentre prospective cohort study

(the SIREN Study). SSRN 3790399 [Preprint]. 22 February 2021. https://papers.ssrn.com/sol3/papers.cfm?abstract_id=3790399.
10. J. M. Dan, J. Mateus, Y. Kato, K. M. Hastie, E. D. Yu, C. E. Faliti, A. Grifoni, S. I. Ramirez, S. Haupt, A. Frazier, C. Nakao, V. Rayaprolu, S. A. Rawlings, B. Peters, F. Krammer, V. Simon, E. O. Saphire, D. M. Smith, D. Weiskopf, A. Sette, S. Crotty, Immunological memory to SARS-CoV-2 assessed for up to 8 months after infection. *Science* **371**, eabf4063 (2021). doi:10.1126/science.abf4063 Medline
11. S. F. Lumley, D. O'Donnell, N. E. Stoesser, P.C. Matthews, A. Howarth, S. B. Hatch, B. D. Marsden, S. Cox, T. James, F. Warren, L. J. Peck, T. G. Ritter, Z. de Toledo, L. Warren, D. Axten, R. J. Cornall, E. Y. Jones, D. I. Stuart, G. Screaton, D. Ebner, S. Hoosdally, M. Chand, Oxford University Hospitals Staff Testing Group, D. W. Crook, A.-M. O'Donnell, C. P. Conlon, K. B. Pouwels, A. S. Walker, T. E. A. Peto, S. Hopkins, T. M. Walker, K. Jeffery, D. W. Eyre, Antibodies to SARS-CoV-2 are associated with protection against reinfection. medRxiv 2020.11.18.20234369 [Preprint]. 19 November 2020. https://doi.org/10.1101/2020.11.18.20234369.
12. A. G. Letizia, I. Ramos, A. Obla, C. Goforth, D. L. Weir, Y. Ge, M. M. Bamman, J. Dutta, E. Ellis, L. Estrella, M.-C. George, A. S. Gonzalez-Reiche, W. D. Graham, A. van de Guchte, R. Gutierrez, F. Jones, A. Kalomoiri, R. Lizewski, S. Lizewski, J. Marayag, N. Marjanovic, E. V. Millar, V. D. Nair, G. Nudelman, E. Nunez, B. L. Pike, C. Porter, J. Regeimbal, S. Rirak, E. Santa Ana, R. S. G. Sealfon, R. Sebra, M. P. Simons, A. Soares-Schanoski, V. Sugiharto, M. Termini, S. Vangeti, C. Williams, O. G. Troyanskaya, H. van Bakel, S. C. Sealfon, SARS-CoV-2 transmission among marine recruits during quarantine. *N. Engl. J. Med.* **383**, 2407–2416 (2020). doi:10.1056/NEJMoa2029717 Medline
13. C. M. Saad-Roy, C. E. Wagner, R. E. Baker, S. E. Morris, J. Farrar, A. L. Graham, S. A. Levin, M. J. Mina, C. J. E. Metcalf, B. T. Grenfell, Immune life history, vaccination, and the dynamics of SARS-CoV-2 over the next 5 years. *Science* **370**, 811–818 (2020). doi:10.1126/science.abd7343 Medline
14. E. Volz, V. Hill, J. T. McCrone, A. Price, D. Jorgensen, Á. O'Toole, J. Southgate, R. Johnson, B. Jackson, F. F. Nascimento, S. M. Rey, S. M. Nicholls, R. M. Colquhoun, A. da Silva Filipe, J. Shepherd, D. J. Pascall, R. Shah, N. Jesudason, K. Li, R. Jarrett, N. Pacchiarini, M. Bull, L. Geidelberg, I. Siveroni, I. Goodfellow, N. J. Loman, O. G. Pybus, D. L. Robertson, E. C. Thomson, A. Rambaut, T. R. Connor; COG-UK Consortium, Evaluating the effects of SARS-CoV-2 Spike mutation D614G on transmissibility and pathogenicity. *Cell* **184**, 64–75.e11 (2021). doi:10.1016/j.cell.2020.11.020 Medline
15. A. M. Gravagnuolo, L. Faqih, C. Cronshaw, J. Wynn, L. Burglin, P. Klapper, M. Wigglesworth, Epidemiological investigation of new SARS-CoV-2 variant of concern 202012/01 in England. medRxiv 2021.01.14.21249386 [Preprint]. 15 January 2021. https://doi.org/10.1101/2021.01.14.21249386.
16. N. G. Davies, R. C. Barnard, C. I. Jarvis, A. J. Kucharski, J. Munday, C. A. B. Pearson, T. W. Russell, D. C. Tully, S. Abbott, A. Gimma, W. Waites, K. L. M. Wong, K. van Zandvoort, CMMID COVID-19 Working Group, R. M. Eggo, S. Funk, M. Jit, K. E. Atkins, W. J. Edmunds, Estimated transmissibility and severity of novel SARS-CoV-2 variant of concern 202012/01 in England. medRxiv 2020.12.24.20248822 [Preprint]. 26 December 2020. https://doi.org/10.1101/2020.12.24.20248822.
17. B. T. Grenfell, O. G. Pybus, J. R. Gog, J. L. N. Wood, J. M. Daly, J. A. Mumford, E. C. Holmes, Unifying the epidemiological and evolutionary dynamics of pathogens. *Science* **303**, 327–332 (2004). doi:10.1126/science.1090727 Medline
18. R. Eguia, K. H. D. Crawford, T. Stevens-Ayers, L. Kelnhofer-Millevolte, A. L. Greninger, J. A. Englund, M. J. Boeckh, J. D. Bloom, A human coronavirus evolves antigenically to escape antibody immunity. bioRxiv 2020.12.17.423313 [Preprint]. 18 December 2020. https://doi.org/10.1101/2020.12.17.423313.
19. S. R. Kadire, R. M. Wachter, N. Lurie, Delayed second dose versus standard regimen for Covid-19 vaccination. *N. Engl. J. Med.* **384**, e28 (2021). doi:10.1056/NEJMcIde2101987 Medline
20. S. E. Morris, V. E. Pitzer, C. Viboud, C. J. E. Metcalf, O. N. Bjørnstad, B. T. Grenfell, Demographic buffering: Titrating the effects of birth rate and imperfect immunity on epidemic dynamics. *J. R. Soc. Interface* **12**, 20141245 (2015). doi:10.1098/rsif.2014.1245 Medline
21. R. E. Baker, W. Yang, G. A. Vecchi, C. J. E. Metcalf, B. T. Grenfell, Susceptible supply limits the role of climate in the early SARS-CoV-2 pandemic. *Science* **369**, 315–319 (2020). doi:10.1126/science.abc2535 Medline
22. C. M. Saad-Roy, S. A. Levin, C. J. E. Metcalf, B. T. Grenfell, Trajectory of individual immunity and vaccination required for SARS-CoV-2 community immunity: A conceptual investigation. *J. R. Soc. Interface* **18**, 20200683 (2021). doi:10.1098/rsif.2020.0683 Medline
23. C. E. Wagner, J. A. Prentice, C. M. Saad-Roy, L. Yang, B. T. Grenfell, S. A. Levin, R. Laxminarayan, Economic and behavioral influencers of vaccination and antimicrobial use. *Front. Public Health* **8**, 614113 (2020). doi:10.3389/fpubh.2020.614113 Medline
24. H. Tegally, E. Wilkinson, M. Giovanetti, A. Iranzadeh, V. Fonseca, J. Giandhari, D. Doolabh, S. Pillay, E. J. San, N. Msomi, K. Mlisana, A. von Gottberg, S. Walaza, M. Allam, A. Ismail, T. Mohale, A. J. Glass, S. Engelbrecht, G. Van Zyl, W. Preiser, F. Petruccione, A. Sigal, D. Hardie, G. Marais, M. Hsiao, S. Korsman, M.-A. Davies, L. Tyers, I. Mudau, D. York, C. Maslo, D. Goedhals, S. Abrahams, O. Laguda-Akingba, A. Alisoltani-Dehkordi, A. Godzik, C. K. Wibmer, B. T. Sewell, J. Lourenço, L. C. J. Alcantara, S. L. Kosakovsky Pond, S. Weaver, D. Martin, R. J. Lessells, J. N. Bhiman, C. Williamson, T. de Oliveira, Emergence and rapid spread of a new severe acute respiratory syndrome-related coronavirus 2 (SARS-CoV-2) lineage with multiple spike mutations in South Africa. medRxiv 2020.12.21.20248640 [Preprint]. 22 December 2020. https://doi.org/10.1101/2020.12.21.20248640.
25. N. R. Faria, I. Morales Claro, D. Candido, L. A. Moyses Franco, P. S. Andrade, T. M. Coletti, C. A. M. Silva, F. C. Sales, E. R. Manuli, R. S. Aguiar, N. Gaburo, C. da C. Camilo, N. A. Fraiji, M. A. Esashika Crispim, M. do Perpétuo S. S. Carvalho, A. Rambaut, N. Loman, O. G. Pybus, E. C. Sabino, CADDE Genomic Network, "Genomic characterisation of an emergent SARS-CoV-2 lineage in Manaus: preliminary findings," Virological.org (2021); https://virological.org/t/genomic-characterisation-of-an-emergent-sars-cov-2-lineage-in-manaus-preliminary-findings/586.
26. A. Rambaut, N. Loman, O. Pybus, W. Barclay, J. Barrett, A. Carabelli, T. Connor, T. Peacock, D. L. Robertson, E. Volz, COVID-19 Genomics Consortium UK (CoG-UK), "Preliminary genomic characterisation of an emergent SARS-CoV-2 lineage in the UK defined by a novel set of spike mutations," Virological.org (2020); https://virological.org/t/preliminary-genomic-characterisation-of-an-emergent-sars-cov-2-lineage-in-the-uk-defined-by-a-novel-set-of-spike-mutations/563.
27. I. F. Miller, C. J. E. Metcalf, No current evidence for risk of vaccine-driven virulence evolution in SARS-CoV-2. medRxiv 2020.12.01.20241836 [Preprint]. 3 December 2020. https://doi.org/10.1101/2020.12.01.20241836.
28. E. J. Emanuel, G. Persad, A. Kern, A. Buchanan, C. Fabre, D. Halliday, J. Heath, L. Herzog, R. J. Leland, E. T. Lemango, F. Luna, M. S. McCoy, O. F. Norheim, T. Ottersen, G. O. Schaefer, K.-C. Tan, C. H. Wellman, J. Wolff, H. S. Richardson, An ethical framework for global vaccine allocation. *Science* **369**, 1309–1312 (2020). doi:10.1126/science.abe2803 Medline
29. T. Burki, Equitable distribution of COVID-19 vaccines. *Lancet Infect. Dis.* **21**, 33–34 (2021). doi:10.1016/S1473-3099(20)30949-X Medline
30. J. S. Lavine, O. N. Bjornstad, R. Antia, Immunological characteristics govern the transition of COVID-19 to endemicity. *Science* **371**, 741–745 (2021). doi:10.1126/science.abe6522 Medline
31. K. Sun, W. Wang, L. Gao, Y. Wang, K. Luo, L. Ren, Z. Zhan, X. Chen, S. Zhao, Y. Huang, Q. Sun, Z. Liu, M. Litvinova, A. Vespignani, M. Ajelli, C. Viboud, H. Yu, Transmission heterogeneities, kinetics, and controllability of SARS-CoV-2. *Science* **371**, eabe2424 (2021). doi:10.1126/science.abe2424 Medline
32. R. Laxminarayan, B. Wahl, S. R. Dudala, K. Gopal, C. Mohan B, S. Neelima, K. S. Jawahar Reddy, J. Radhakrishnan, J. A. Lewnard, Epidemiology and transmission dynamics of COVID-19 in two Indian states. *Science* **370**, 691–697 (2020). doi:10.1126/science.abd7672 Medline
33. D. C. Adam, P. Wu, J. Y. Wong, E. H. Y. Lau, T. K. Tsang, S. Cauchemez, G. M. Leung, B. J. Cowling, Clustering and superspreading potential of SARS-CoV-2 infections in Hong Kong. *Nat. Med.* **26**, 1714–1719 (2020). doi:10.1038/s41591-020-1092-0 Medline
34. M. Voysey, S. A. Costa Clemens, S. A. Madhi, L. Y. Weckx, P. M. Folegatti, P. K. Aley, B. J. Angus, V. Baillie, S. L. Barnabas, Q. E. Bhorat, S. Bibi, C. Briner, P. Cicconi, E. Clutterbuck, A. M. Collins, C. Cutland, T. Darton, K. Dheda, A. D. Douglas, C. J. A. Duncan, K. R. W. Emary, K. Ewer, A. Flaxman, L. Fairlie, S. N. Faust, S. Feng, D. M. Ferreira, A. Finn, E. Galiza, A. L. Goodman, C. M. Green, C. A. Green, M. Greenland, C. Hill, H. C. Hill, I. Hirsch, A. Izu, D. Jenkin, S. Kerridge, A. Koen, G. Kwatra, R. Lazarus, V. Libri, P. J. Lillie, N. G. Marchevsky, R. P. Marshall, A. V. A. Mendes, E. P. Milan, A. M. Minassian, A. C. McGregor, Y. Farooq Mujadidi, A. Nana, S. D.

Payadachee, D. J. Phillips, A. Pittella, E. Plested, K. M. Pollock, M. N. Ramasamy, H. Robinson, A. V. Schwarzbold, A. Smith, R. Song, M. D. Snape, E. Sprinz, R. K. Sutherland, E. C. Thomson, M. Torok, M. Toshner, D. P. J. Turner, J. Vekemans, T. L. Villafana, T. White, C. J. Williams, A. V. S. Hill, T. Lambe, S. C. Gilbert, A. Pollard, Oxford COVID Vaccine Trial Group, Single dose administration, and the influence of the timing of the booster dose on immunogenicity and efficacy of ChAdOx1 nCoV-19 (AZD1222) vaccine. SSRN 3777268 [Preprint]. 1 February 2021. https://papers.ssrn.com/sol3/papers.cfm?abstractid=3777268.

35. L. F. Buss, C. A. Prete Jr., C. M. M. Abrahim, A. Mendrone Jr., T. Salomon, C. de Almeida-Neto, R. F. O. França, M. C. Belotti, M. P. S. S. Carvalho, A. G. Costa, M. A. E. Crispim, S. C. Ferreira, N. A. Fraiji, S. Gurzenda, C. Whittaker, L. T. Kamaura, P. L. Takecian, P. da Silva Peixoto, M. K. Oikawa, A. S. Nishiya, V. Rocha, N. A. Salles, A. A. de Souza Santos, M. A. da Silva, B. Custer, K. V. Parag, M. Barral-Netto, M. U. G. Kraemer, R. H. M. Pereira, O. G. Pybus, M. P. Busch, M. C. Castro, C. Dye, V. H. Nascimento, N. R. Faria, E. C. Sabino, Three-quarters attack rate of SARS-CoV-2 in the Brazilian Amazon during a largely unmitigated epidemic. *Science* **371**, 288–292 (2021). doi:10.1126/science.abe9728 Medline
36. M. G. Baker, N. Wilson, A. Anglemyer, Successful elimination of Covid-19 transmission in New Zealand. *N. Engl. J. Med.* **383**, e56 (2020). doi:10.1056/NEJMc2025203 Medline
37. D. J. Summers, D. H.-Y. Cheng, P. H.-H. Lin, D. L. T. Barnard, D. A. Kvalsvig, P. N. Wilson, P. M. G. Baker, Potential lessons from the Taiwan and New Zealand health responses to the COVID-19 pandemic. *Lancet Reg. Health West. Pac.* **4**, 100044 (2020). doi:10.1016/j.lanwpc.2020.100044
38. COVID-19 National Incident Room Surveillance Team, Epidemiology Report 31: Fortnightly reporting period ending 6 December 2020. *Commun. Dis. Intell.* **44**, 10.33321/cdi.2020.44.92 (2020). 10.33321/cdi.2020.44.92
39. Epidemiological and evolutionary dynamics of SARS-CoV-2 interactive dashboard, http://grenfelllab.princeton.edu/sarscov2vaccine.
40. N. M. Ferguson, A. P. Galvani, R. M. Bush, Ecological and immunological determinants of influenza evolution. *Nature* **422**, 428–433 (2003). doi:10.1038/nature01509 Medline
41. K. Koelle, S. Cobey, B. Grenfell, M. Pascual, Epochal evolution shapes the phylodynamics of interpandemic influenza A (H3N2) in humans. *Science* **314**, 1898–1903 (2006). doi:10.1126/science.1132745 Medline
42. B. Choi, M. C. Choudhary, J. Regan, J. A. Sparks, R. F. Padera, X. Qiu, I. H. Solomon, H.-H. Kuo, J. Boucau, K. Bowman, U. D. Adhikari, M. L. Winkler, A. A. Mueller, T. Y.-T. Hsu, M. Desjardins, L. R. Baden, B. T. Chan, B. D. Walker, M. Lichterfeld, M. Brigl, D. S. Kwon, S. Kanjilal, E. T. Richardson, A. H. Jonsson, G. Alter, A. K. Barczak, W. P. Hanage, X. G. Yu, G. D. Gaiha, M. S. Seaman, M. Cernadas, J. Z. Li, Persistence and evolution of SARS-CoV-2 in an immunocompromised host. *N. Engl. J. Med.* **383**, 2291–2293 (2020). doi:10.1056/NEJMc2031364 Medline
43. D. H. Morris, V. N. Petrova, F. W. Rossine, E. Parker, B. T. Grenfell, R. A. Neher, S. A. Levin, C. A. Russell, Asynchrony between virus diversity and antibody selection limits influenza virus evolution. *eLife* **9**, e62105 (2020). doi:10.7554/eLife.62105 Medline
44. J. Gog, Vaccine Escape: Exploring the simplest model; https://sms.cam.ac.uk/media/3436478.
45. K. M. Pepin, I. Volkov, J. R. Banavar, C. O. Wilke, B. T. Grenfell, Phenotypic differences in viral immune escape explained by linking within-host dynamics to host-population immunity. *J. Theor. Biol.* **265**, 501–510 (2010). doi:10.1016/j.jtbi.2010.05.036 Medline
46. J. Zahradn, S. Marciano, M. Shemesh, E. Zoler, J. Chiaravalli, B. Meyer, Y. Rudich, O. Dym, N. Elad, G. Schreiber, SARS-CoV-2 RBD in vitro evolution follows contagious mutation spread, yet generates an able infection inhibitor. bioRxiv 2021.01.06.425392 [Preprint]. 6 January 2021. https://doi.org/10.1101/2021.01.06.425392.
47. E. M. Volz, K. Koelle, T. Bedford, Viral phylodynamics. *PLOS Comput. Biol.* **9**, e1002947 (2013). doi:10.1371/journal.pcbi.1002947 Medline
48. R. Biek, O. G. Pybus, J. O. Lloyd-Smith, X. Didelot, Measurably evolving pathogens in the genomic era. *Trends Ecol. Evol.* **30**, 306–313 (2015). doi:10.1016/j.tree.2015.03.009 Medline
49. C. Baraniuk, Covid-19: How the UK vaccine rollout delivered success, so far. *BMJ* **372**, n421 (2021). doi:10.1136/bmj.n421 Medline
50. S. A. Madhi, V. Baillie, C. L. Cutland, M. Voysey, A. L. Koen, L. Fairlie, S. D. Padayachee, K. Dheda, S. L. Barnabas, Q. E. Bhorat, C. Briner, G. Kwatra, NGS-SA, Wits-VIDA COVID team, K. Ahmed, P. Aley, S. Bhikha, J. N. Bhiman, A. Ebrahim Bhorat, J. du Plessis, A. Esmail, M. Groenewald, E. Horne, S.-H. Hwa, A. Jose, T. Lambe, M. Laubscher, M. Malahleha, M. Masenya, M. Masilela, S. McKenzie, K. Molapo, A. Moultrie, S. Oelofse, F. Patel, S. Pillay, S. Rhead, H. Rodel, L. Rossouw, C. Taoushanis, H. Tegally, A. Thombrayil, S. van Eck, C. K. Wibmer, N. M. Durham, E. J. Kelly, T. L. Villafana, S. Gilbert, A. J. Pollard, T. de Oliveira, P. L. Moore, A. Sigal, A. Izu, Safety and efficacy of the ChAdOx1 nCoV-19 (AZD1222) Covid-19 vaccine against the B.1.351 variant in South Africa. medRxiv 2021.02.10.21251247 [Preprint]. 12 February 2021. https://doi.org/10.1101/2021.02.10.21251247.
51. C. M. Saad-Roy, A. B. McDermott, B. T. Grenfell, Dynamic perspectives on the search for a universal influenza vaccine. *J. Infect. Dis.* **219** (suppl. 1), S46–S56 (2019). doi:10.1093/infdis/jiz044 Medline
52. E. M. Volz, S. L. Kosakovsky Pond, M. J. Ward, A. J. Leigh Brown, S. D. W. Frost, Phylodynamics of infectious disease epidemics. *Genetics* **183**, 1421–1430 (2009). doi:10.1534/genetics.109.106021 Medline
53. S. M. Kissler, C. Tedijanto, E. Goldstein, Y. H. Grad, M. Lipsitch, Projecting the transmission dynamics of SARS-CoV-2 through the postpandemic period. *Science* **368**, 860–868 (2020). doi:10.1126/science.abb5793 Medline
54. J. Zhang, M. Litvinova, W. Wang, Y. Wang, X. Deng, X. Chen, M. Li, W. Zheng, L. Yi, X. Chen, Q. Wu, Y. Liang, X. Wang, J. Yang, K. Sun, I. M. Longini Jr., M. E. Halloran, P. Wu, B. J. Cowling, S. Merler, C. Viboud, A. Vespignani, M. Ajelli, H. Yu, Evolving epidemiology and transmission dynamics of coronavirus disease 2019 outside Hubei province, China: A descriptive and modelling study. *Lancet Infect. Dis.* **20**, 793–802 (2020). doi:10.1016/S1473-3099(20)30230-9 Medline
55. R. E. Baker, A. S. Mahmud, C. E. Wagner, W. Yang, V. E. Pitzer, C. Viboud, G. A. Vecchi, C. J. E. Metcalf, B. T. Grenfell, Epidemic dynamics of respiratory syncytial virus in current and future climates. *Nat. Commun.* **10**, 5512 (2019). doi:10.1038/s41467-019-13562-y Medline
56. We qualitatively describe the fraction of population that have received vaccines by assuming that vaccination occurs at random in the population. Specifically, suppose vaccination occurs at time $\tau = 0$. The rate of change of the fraction not vaccinated follows $\frac{dN}{d\tau} = -\nu N$, $N(0) = 1$, giving $N(\tau) = e^{-\nu\tau}$ so that the fraction vaccinated with one dose $Y(\tau) = 1 - N(\tau) = 1 - e^{-\nu\tau}$. The fractions of those vaccinated with one but not two doses follows $\frac{dW_1}{d\tau} = \nu N - \omega W_1$, giving $W_1(\tau) = \frac{\nu\left(e^{-\nu\tau} - e^{-\omega\tau}\right)}{\omega - \nu}$. Then, the fraction vaccinated with two doses is $W_2(\tau) = Y(\tau) - W_1(\tau) = 1 - \frac{\omega}{\omega - \nu}e^{-\nu\tau} + \frac{\nu}{\omega - \nu}e^{-\omega\tau}$.
57. We calculate the total number of cases at any time point as $I_T = I_P + I_S + I_V + I_{S_1} + I_{S_2}$. Similarly, the number of severe cases is given by $I_{T,\text{sev}} = x_{\text{sev},p}I_P + x_{\text{sev},s}I_S + x_{\text{sev},V}I_V + x_{\text{sev},1}I_{S_1} + x_{\text{sev},2}I_{S_2}$. Cumulative case numbers for a give time period are calculated through $\gamma\sum I_T$ (total cases) and $\gamma\sum I_{T,\text{sev}}$ (severe cases), where the summation occurs over all time steps.
58. C. M. Saad-Roy, S. E. Morris, C. J. E. Metcalf, M. J. Mina, R. E. Baker, J. Farrar, E. C. Holmes, O. G. Pybus, A. L. Graham, S. A. Levin, B. T. Grenfell, C. E. Wagner, Code for Epidemiological and evolutionary considerations of SARS-CoV-2 vaccine dosing regimes, Version 1, Zenodo (2021); https://doi.org/10.5281/zenodo.4556111.
59. O. Diekmann, J. A. P. Heesterbeek, J. A. J. Metz, On the definition and the computation of the basic reproduction ratio R_0 in models for infectious diseases in heterogeneous populations. *J. Math. Biol.* **28**, 365–382 (1990). doi:10.1007/BF00178324 Medline
60. P. van den Driessche, J. Watmough, Reproduction numbers and sub-threshold endemic equilibria for compartmental models of disease transmission. *Math.*

Biosci. **180**, 29–48 (2002). doi:10.1016/S0025-5564(02)00108-6 Medline
61. R. M. Anderson, R. M. May, *Infectious Diseases of Humans: Dynamics and Control* (Oxford Univ. Press, 1992).
62. T. Britton, F. Ball, P. Trapman, A mathematical model reveals the influence of population heterogeneity on herd immunity to SARS-CoV-2. *Science* **369**, 846–849 (2020). doi:10.1126/science.abc6810 Medline
63. R. M. May, R. M. Anderson, Spatial heterogeneity and the design of immunization programs. *Math. Biosci.* **72**, 83–111 (1984). doi:10.1016/0025-5564(84)90063-4
64. S. C. Hadler, M. A. de Monzon, D. R. Lugo, M. Perez, Effect of timing of hepatitis B vaccine doses on response to vaccine in Yucpa Indians. *Vaccine* **7**, 106–110 (1989). doi:10.1016/0264-410X(89)90046-7 Medline

ACKNOWLEDGMENTS

Funding: This work was funded in part by Open Philanthropy, the Natural Sciences and Engineering Research Council of Canada through a Postgraduate-Doctoral Scholarship (C.M.S.-R.), the Cooperative Institute for Modelling the Earth System (CIMES) (R.E.B.), the James S. McDonnell Foundation 21st Century Science Initiative Collaborative Award in Understanding Dynamic and Multi-scale Systems (C.M.S.-R., S.A.L.), the C3.ai Digital Transformation Institute and Microsoft Corporation (S.A.L.), Gift from Google, LLC (S.A.L.), the National Science Foundation (CNS-2027908, CCF1917819) (S.A.L.), the U.S. CDC (B.T.G.), Flu Lab (B.T.G.). **Author contributions:** C.M.S.-R., C.E.W., and B.T.G. designed the study. C.M.S.-R. and C.E.W. performed the simulations and analyses, and wrote the manuscript. S.E.M. developed the Shiny application. All authors contributed to interpreting the results and editing the manuscript. **Competing interests:** The authors have no competing interests. **Data and materials availability:** This manuscript contains no new data, and all referenced data sets are publicly available. Code for all analyses is available at Zenodo (*58*).

SUPPLEMENTARY MATERIALS

science.sciencemag.org/cgi/content/full/science.abg8663/DC1
Supplementary Text
Figs. S1 to S14
References (*59*–*64*)
MDAR Reproducibility Checklist

1 February 2021; accepted 4 March 2021
Published online 9 March 2021
10.1126/science.abg8663

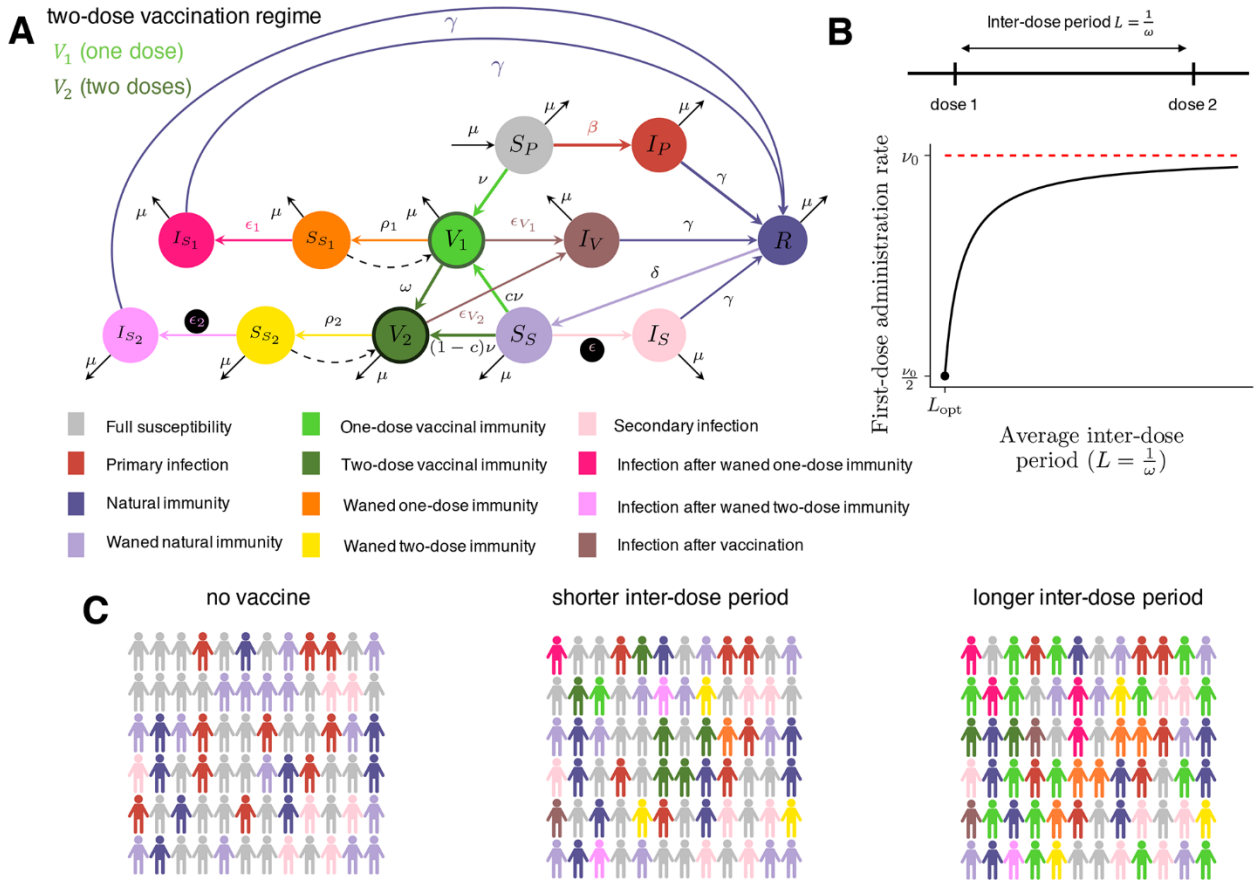

Fig. 1. Description of the extended immuno-epidemiological model with one- and two-dose vaccination regimes [based on (*13*)]. (**A**) Model flow chart depicting transitions between immune classes (see main text and Materials and methods for a full description of the immune classes and parameters). (**B**) Diagram of the inter-dose period $\left(\frac{1}{\omega}\right)$ considered between the first and second vaccine doses and its relationship to the rate of administration of the first vaccine dose ν. The maximum achievable rate is ν_0 for a fully one-dose strategy, and ν is assumed to decrease exponentially to its lowest value $\nu_0/2$ when a fully two-dose strategy with inter-dose period corresponding to the clinical recommendation (L_{opt}) is employed. (**C**) Representative schematic of societal composition of various immune classes for the SIR(S) model with no vaccination (left), the extended model with a short inter-dose period (middle), and the extended model with a long inter-dose period (right).

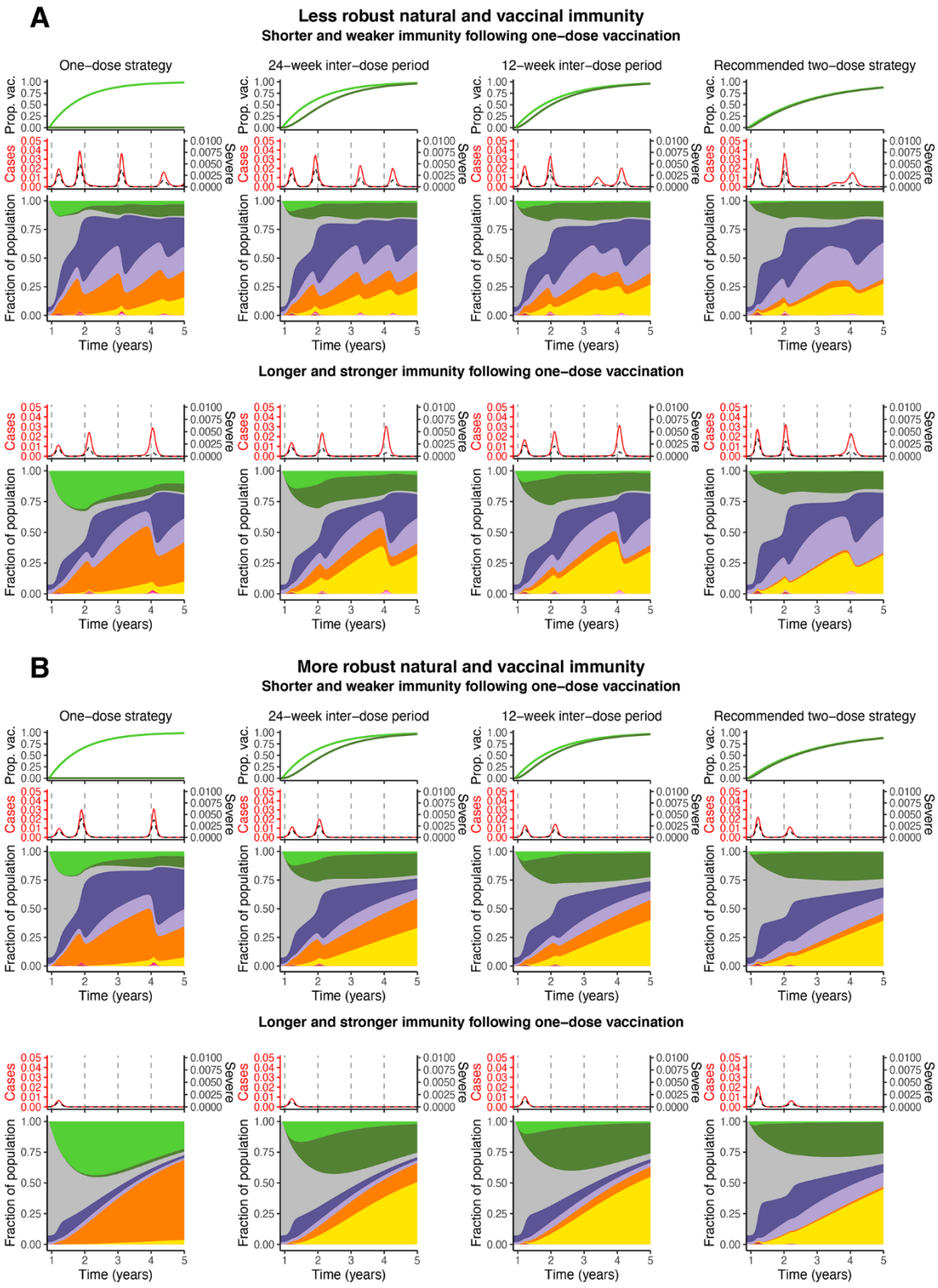

Fig. 2. Synoptic medium-term immune landscapes and infection burden. The immune and infection class colors are the same as those defined in Fig. 1A. For each panel, (top) illustrative time series of the fraction of the population vaccinated with one or two doses [see note (*56*)], (middle) the fraction of total and severe infections [see (*57*)], and (bottom) area plots of the fraction of the population comprising each immune (S_P, R, S_S, V_1, V_2, S_{S_1}, S_{S_2}) or infection (I_P, I_S, I_V, I_{S_1}, I_{S_2}) class from just before the introduction of vaccination until 5 years after the pandemic onset. In all plots, the maximum rate of administration of the first vaccine dose is taken to be ν_0 = 2% and the vaccine is introduced at t_{vax} = 48 weeks. We take $\epsilon_{V_1} = 0.1$ and $\epsilon_{V_2} = 0.05$ in keeping with data from clinical trials (*3*). The fraction of severe cases for primary infections, secondary infections, infection after vaccination, and infection after waned two-dose immunity are taken to be $x_{\text{sev},p} = 0.14$, $x_{\text{sev},s} = 0.07$, $x_{\text{sev},V} = 0.14$, and $x_{\text{sev},2} = 0$. The transmission rates and periods of NPI adoption are defined in the Materials and methods. The leftmost column corresponds to a one-dose vaccine strategy (ω = 0), followed by inter-dose spacings of 24 weeks, 12 weeks, and 4 weeks (rightmost column). (**A**) corresponds to an overall more pessimistic natural and vaccinal immunity scenario, with $\epsilon = \epsilon_2$ = 0.7 and $1/\delta = 1/\rho_2$ = 1 year. For a less effective one-dose vaccine (top section), we take ϵ_1 = 0.9, $1/\rho_1$ = 0.25 years, and the fraction of severe cases associated with infection after waned one-dose immunity is $x_{\text{sev},1} = 0.14$. For an effective one-dose vaccine (bottom section), we take ϵ_1 = 0.7, $1/\rho_1$ = 1 year, and the fraction of severe cases associated with infection after waned one-dose immunity is $x_{\text{sev},1} = 0$. (**B**) corresponds to an overall more optimistic natural and vaccinal immunity scenario, with $\epsilon = \epsilon_2$ = 0.5 and $1/\delta = 1/\rho_2$ = 2 years. For a less effective one-dose vaccine (top section), we take ϵ_1 = 0.9, $1/\rho_1$ = 0.5, $1/\rho_1$ = 0.5 years, and the fraction of severe cases associated with infection after waned one-dose immunity is $x_{\text{sev},1} = 0.14$. For an effective one-dose vaccine (bottom section), we take ϵ_1 = 0.5, $1/\rho_1$ = 2 years, and the fraction of severe cases associated with infection after waned one-dose immunity is $x_{\text{sev},1} = 0$.

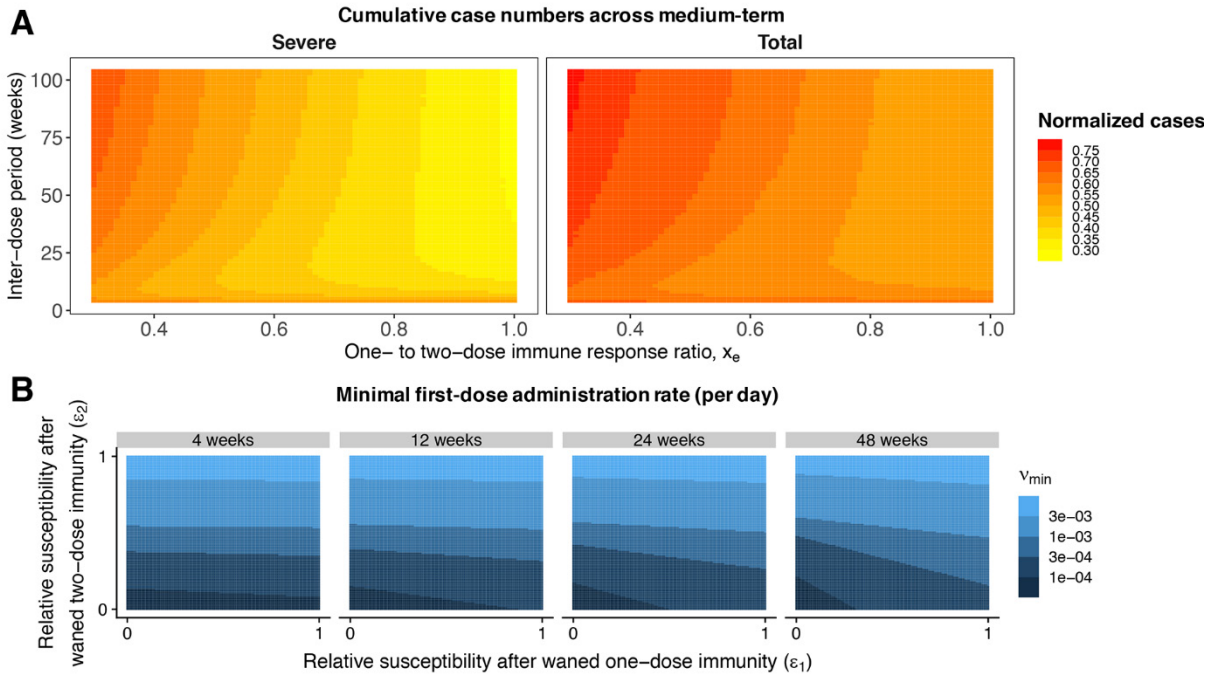

Fig. 3. Heat maps depicting various epidemiological outcomes contingent on dosing regimes. (**A**) Cumulative severe (left) and total (right) case numbers relative to the scenario with no vaccine from the time of vaccine introduction through the end of the five-year time period following the onset of the pandemic as a function of the one- to two-dose immune response ratio x_e and the inter-dose period. Parameters correspond to the "weak" immunity scenario of Fig. 2A, but x_e sets the value of ϵ_1, ρ_1, and $x_{sev,1}$. Specifically, we take $\epsilon_1 = \epsilon_2 + (1 - x_e)(1 - \epsilon_2)$ such that the susceptibility to infection after a waned single dose interpolates linearly between the value after waned two doses (ϵ_2) when the one and two dose immune responses are equally strong ($x_e = 1$) and unity (full susceptibility) when a single dose offers no immune protection ($x_e = 0$). Similarly, we take $x_{sev,1} = x_{sev,2} + (1 - x_e)(x_{sev,V} - x_{sev,2})$ such that the fraction of severe cases for infections following a waned single dose interpolates linearly between the value after waned two doses ($x_{sev,2}$) when $x_e = 1$ and the value after a (failed) vaccination $x_{sev,V}$ when $x_e = 0$. Finally, ρ_1 is given by $\rho_1 = \rho_2/x_e$. (**B**) Values of ν_{min}, the minimal rate of first dose administration per day such that for any $\nu > \nu_{min}$ the basic reproduction $\mathcal{R}_0[\nu] < 1$ and the disease cannot invade (see supplementary materials), as a function of the strength of immunity following one (ϵ_1) and two (ϵ_2) waned vaccines doses, for different inter-dose periods. We take the duration of one dose and two dose vaccinal immunity to be $1/\rho_1 = 0.5$ years and $1/\rho_2 = 1$ year, respectively, and set $\epsilon_{V_1} = 0.1$ and $\epsilon_{V_2} = 0.05$.

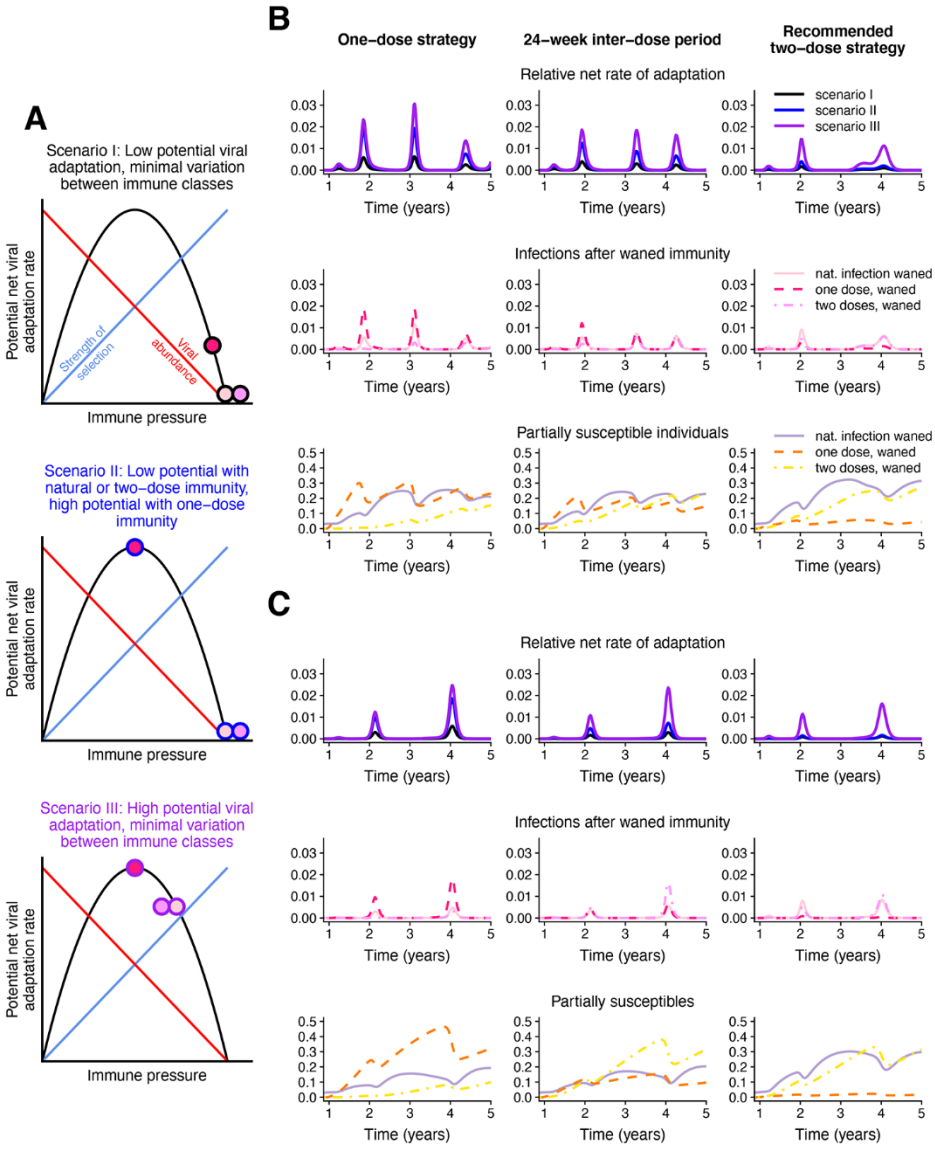

Fig. 4. Potential viral evolution scenarios under different vaccine regimes. (**A**) Schematic representations of the potential net viral adaptation rate associated with the I_S, I_{S_1}, and I_{S_2} infection classes under three different scenarios. These are illustrated by the filled dots, with the central color denoting the infection class and corresponding to the legend in Fig. 1A. The dot outlines correspond to the three scenarios considered (Scenario I: black lines and top panel, Scenario II: blue lines and middle panel, and Scenario III: purple lines and bottom panel). The phylodynamic model for potential viral adaptation as a function of immune pressure is adapted from (*17*). (**B**) and (**C**): Relative net rates of adaptation [top rows; colors correspond to the scenarios in (A)], and composition of associated infection (I_S: solid lines, I_{S_1}: dashed lines, I_{S_2}: dashed-dotted lines; middle rows) and susceptible (S_S: solid lines, S_{S_1}: dashed lines, S_{S_2}: dashed-dotted lines; bottom rows) classes. The colors in the middle and bottom rows correspond to the legend in Fig. 1A. The leftmost column corresponds to a one dose strategy, an inter-dose period of $\frac{1}{\omega} = 24$ weeks is assumed in the middle column, and the rightmost column assumes a two dose strategy with doses separated by the recommended window of $\frac{1}{\omega} = 4$ weeks. Both (B) and (C) correspond to a "weak" natural and vaccinal immunity scenario, with the same parameters as those in Fig. 2A. A weaker immune response after one vaccine dose is assumed in (B) (with parameters corresponding to those in the top section of Fig. 2A), and a stronger immune response after one vaccine dose is assumed in (C) (with parameters corresponding to those in the bottom section of Fig. 2A). The weights used to calculate the relative net rates of adaptation are $w_{IS,I} = 0.05$, $w_{IS1,I} = 0.3$, and $w_{IS2,I} = 0.05$ in Scenario I, $w_{IS,II} = 0.05$, $w_{IS1,II} = 1$, and $w_{IS2,II} = 0.05$ in Scenario II, and $w_{IS,III} = 0.8$, $w_{IS1,III} = 1$, and $w_{IS2,III} = 0.8$ in Scenario III.

Epidemiological and evolutionary considerations of SARS-CoV-2 vaccine dosing regimes

Chadi M. Saad-Roy, Sinead E. Morris, C. Jessica E. Metcalf, Michael J. Mina, Rachel E. Baker, Jeremy Farrar, Edward C. Holmes, Oliver G. Pybus, Andrea L. Graham, Simon A. Levin, Bryan T. Grenfell and Caroline E. Wagner

published online March 9, 2021

Science (print ISSN 0036-8075; online ISSN 1095-9203) is published by the American Association for the Advancement of Science, 1200 New York Avenue NW, Washington, DC 20005. The title *Science* is a registered trademark of AAAS.